

Intensity-resolved multiphoton ionization: Circumventing spatial averaging

M. A. Walker, P. Hansch, and L. D. Van Woerkom

Department of Physics, The Ohio State University, Columbus, Ohio 43210-1106

(Received 19 June 1997; revised manuscript received 29 October 1997)

A persistent problem in traditional high-field photoionization experiments is the intensity averaging caused by the use of focused laser beams. We show that it is possible to deconvolve ionization probabilities directly from data for experiments in which the detection volume is restricted. The inversion technique is outlined and as an example we apply it to multiphoton multiple-ionization measurements of xenon.
[S1050-2947(98)50302-2]

PACS number(s): 32.80.Rm, 32.80.Fb, 32.80.Wr, 42.50.Hz

The study of the ionization of atoms and molecules by strong laser fields relies heavily on measurements of the dependence of many processes on laser intensity. Since the most fundamental physics takes place on the scale of single atoms, the simplest experiment one could imagine would observe the response of a single atom or molecule to a single intensity. Current experiments, however, must sacrifice these optimum conditions if high-field phenomena are to be observed. Pulsed lasers must be used along with focused beams, which implies that the target atoms experience temporal and spatial variations in the laser intensity. The result is that these experiments yield averaged data that reflect not only the essential physics, but also the influence of the experimental configuration and the intensity distribution itself. A natural solution to this problem would be to “undo” the averaging to recover the underlying physics, but this has proven intractable for traditional experiments. This paper will demonstrate that data collected from a modified experimental setup can in fact be deconvolved to remove the averaging using a simple algorithm.

The traditional approach to extracting information from experimental data that reflect spatial averaging has involved two main tactics. The simplest is to approximate the situation as being dominated by the highest intensities near the center of the focus, which is reasonable given the highly nonlinear nature of the processes involved. The other tactic is to incorporate spatial averaging into theoretical models of the experiments, and compare these with the data. These methods have been employed in constructing nearly all of the current body of knowledge of high-intensity photoionization. However, recent work has demonstrated the existence of phenomena that cannot be observed in intensity-averaged data. Talebpour *et al.* [1] employed a loose focus (Rayleigh range ≈ 6 cm) in combination with a 2 cm aperture to observe subtle features in the ion yields of xenon and krypton. Jones [2–4] combined a loose focus with an aperture and time-of-flight selection to achieve complete spatial resolution, revealing the presence of coherence effects in resonant multiphoton ionization of sodium. Hansch *et al.* [5] employed the intensity-selective scanning (ISS) [6] technique to observe charge-state depletion and other effects in multiphoton multiple ionization of xenon, and Schafer and Kulander [7] recently described the prospect of using ISS to observe interference effects in resonant population transfer in xenon. The characteristic common to all of this work is that the volume

from which the ionization products were collected (or calculated) was limited to a small portion of the interaction region over which there was negligible variation in intensity in one or more dimensions. In the case of ISS, the intensity variation along the beam axis direction is removed. In addition, the information gained by scanning the aperture over the focus can be used to unravel the radial averaging. The data from experiments using ISS are thus in a form that can be deconvolved in a few simple steps. The remainder of this paper outlines how this is done and presents an example in the form of ionization probability measurements for xenon.

The traditional experimental setup used in time-of-flight measurements, which shall be referred to here as “full view,” involves exposing the entire interaction region to the detector. Intensity-dependent processes are observed by varying the overall power of the laser beam using filters or polarization techniques. The beam is focused into the center of the interaction region by a lens or mirror, which produces an axisymmetric spatial distribution of temporal peak intensities. Ionization takes place throughout the focal volume given by

$$I(r, z) = \frac{I_0}{1 + (z/z_0)^2} \exp\left(-\frac{r^2}{\omega_0^2[1 + (z/z_0)^2]}\right), \quad (1)$$

where I_0 is the maximum peak intensity, ω_0 is the minimum beam waist of the electric field, and z_0 is the Rayleigh range defined by $z_0 = \pi\omega_0^2/\lambda$. The measured signal $S_{FV}(I_0)$, i.e., the number of electrons of a given kinetic energy or ions of a particular q/m that reach the detector, is measured as a function of I_0 , the on-axis temporal peak intensity at the beam waist. Since there are no constraints on which regions of the focus can contribute to the signal (except perhaps for the flight tube aperture itself), all regions, and hence all the intensities present in these regions, will contribute.

By contrast, the ISS method uses a pinhole placed near the focus, between it and the detector, to limit the volume seen by the detector to a thin “slice” through the beam perpendicular to its propagation (z) axis. This slice is “thin” in the sense that there is little variation in the on-axis intensity across its width; specifically Δz , the slit width, is small compared to the Rayleigh range, z_0 . The overall intensity I_0 is kept fixed at the maximum, and different on-axis “local” peak intensities where $I_{0L}(z) = I_0(1 + z^2/z_0^2)^{-1}$ are selected

by varying the z position of the pinhole. The signal collected, S_{ISS} , can be represented either as a function of z or of $I_{0L}(z)$.

Both full view and ISS experiments sample enough of the focus that there is intensity averaging present in their results. An examination of the general nature of this averaging as well as its specific form for each scheme illustrates the deconvolution problem and how it is dealt with through the use of ISS. In a spatial representation the generic expression for the signal from a spatially averaged experiment is

$$S = \int N(I(\vec{r})) d^3r = 2\pi \int \int N(I(r, z)) r dr dz, \quad (2)$$

where the integration limits depend on the details of the experiment. Here $N(I)$ is the fundamental quantity; for example, the fraction of neutral atoms ionized by a given intensity. $N(I)$ acquires an implicit space dependence through the intensity, and this spatially dependent signal is integrated over the relevant volume. For full view, the integral extends essentially over all space, whereas for ISS only a small interval in z is spanned:

$$S_{\text{FV}}(I_0) = 2\pi \int_{-\infty}^{\infty} dz \int_0^{\infty} N(I(I_0, r, z)) r dr, \quad (3)$$

$$S_{\text{ISS}}(z) = 2\pi \Delta z \int_0^{\infty} N(I(r, z)) r dr.$$

The consequences of this accumulation of signal are best examined in an intensity representation, where the averaging takes the following form:

$$S(I_0) = \int N(I) dV(I, I_0) = \int_0^{I_0} N(I) K(I, I_0) dI, \quad (4)$$

where

$$K(I, I_p) = \left| \frac{\partial V}{\partial I} (I, I_p) \right|. \quad (5)$$

Here I_p is the experimental intensity parameter (I_0 for full view, I_{0L} for ISS) and $dV(I, I_p)$ is the real-space volume occupied by intensities between I and $I + dI$ for a given value of I_p . For full view, $V(I, I_0)$ has the form [8]

$$V_{\text{FV}}(I, I_0) = \pi z_0 \omega_0^2 \left\{ \frac{4}{3} \left[\frac{I_0 - I}{I} \right]^{1/2} + \frac{2}{9} \left[\frac{I_0 - I}{I} \right]^{3/2} - \frac{4}{3} \tan^{-1} \left[\frac{I_0 - I}{I} \right]^{1/2} \right\}, \quad (6)$$

whereas for ISS the form of $V(I, I_{0L})$ reduces to [9]

$$V_{\text{ISS}}(I, I_{0L}) = \frac{1}{2} \pi \omega_0^2 \Delta z \left(\frac{I_0}{I_{0L}} \right) \ln \left(\frac{I_{0L}}{I} \right). \quad (7)$$

In real space, $V(I, I_p)$ is the volume bounded by the curve $I(I_p, r, z) = \text{const.}$ The peanutlike shape of a typical $V_{\text{FV}}(I, I_0)$ is shown in Fig. 1(a). Also indicated in this figure is a “slice” of this volume at $z = c$, which constitutes $V_{\text{ISS}}(I_0, z = c)$ for the same I_0 . The shape of $V_{\text{ISS}}(I_0, z = c)$

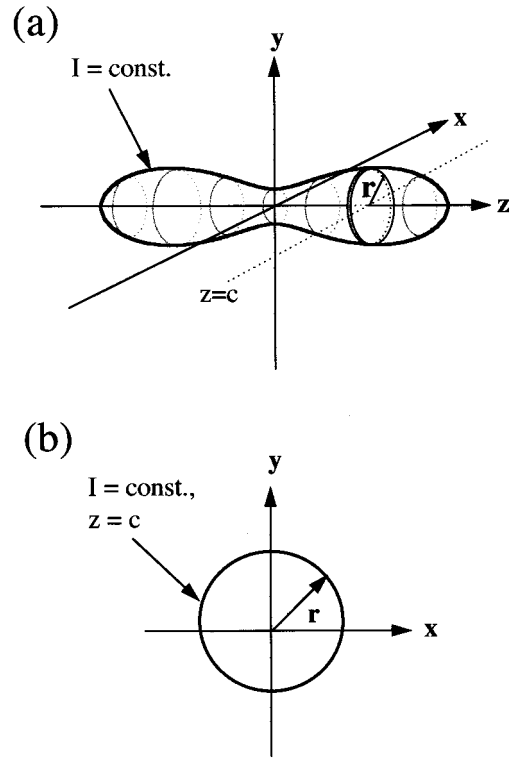


FIG. 1. (a) Example of a typical isointensity contour for the full view case with a small slice representative of an ISS volume shown at $z = c$. (b) The same ISS volume seen in the $z = c$ plane.

in the $z = c$ plane is shown in Fig. 1(b). Detecting only a slice of the focal volume creates a dramatic change in the volumetric weighting of the measured signal. The full Gaussian intensity distribution is reduced to a one-dimensional radial distribution. Thus, a unique one-to-one mapping exists between any radius r and the laser intensity I with local peak intensity $I_{0L}(z)$.

The quantity to be recovered, $N(I)$, is contained inside an integral and therefore we are faced with the problem of solving an integral equation. Within the formal theory of such equations, Eq. (4) can be identified as a linear Volterra equation of the first kind [10]. As might be suspected, the existence of an analytic method for solving such an equation depends critically on the form of the kernel $K(I, I_p)$, which in turn is determined by the intensity distribution and how it is sampled. For full view, $K_{\text{FV}}(I, I_0)$ has the form [8]

$$K_{\text{FV}}(I, I_0) = \frac{\partial V_{\text{FV}}}{\partial I} (I, I_0) = \frac{\pi z_0 \omega_0^2}{3} \frac{2I + I_0}{I} \left[\frac{I_0 - I}{I} \right]^{1/2}. \quad (8)$$

Without going into detail, the equation that results from substitution of Eq. (8) into Eq. (4) can be placed in the form of an Abel equation [10]. Abel equations have been studied in several other applications, including plasma spectroscopy and astrophysics, where measurements made over cylindrical geometries yield similarly averaged results. Though a mathematical solution for the full view case should in principle exist, in practice, its implementation has not proven feasible. Theoretical treatments have therefore resorted to using Eq. (4) along with a model of $N(I)$ to construct $S_{\text{FV}}(I_0)$ for a

comparison to experiment. The weakness of this approach is that it sacrifices information about the detailed behavior of $N(I)$ through the filtering effects of $K(I, I_0)$. Interpretation of the results is less intuitive since complex geometric factors must be considered in addition to the relevant physics.

The form of the kernel for the ISS case, however, is much simpler and the inversion turns out to be trivial. Differentiating Eq. (7) yields

$$K_{\text{ISS}}(I, I_{0L}(z)) = \frac{1}{2} \pi z_0 \omega_0^2 \Delta z \frac{I_0}{I_{0L}(z)} \frac{1}{I}, \quad (9)$$

which when inserted into Eq. (4) gives

$$S_{\text{ISS}}(z) = \frac{1}{2} \pi z_0 \omega_0^2 \Delta z \frac{I_0}{I_{0L}(z)} \int_0^{I_{0L}(z)} \frac{N(I)}{I} dI. \quad (10)$$

Here, S_{ISS} is represented as a function of z , since this is how the data are collected, and therefore the inversion is most direct if applied to this form. This equation can be inverted by multiplying both sides by $I_{0L}(z)$, differentiating with respect to z , and applying the Liebniz rule [11]:

$$N(I_{0L}(z)) \propto \left[\frac{I_{0L}(z)}{dI_{0L}(z)/dz} \right] \frac{d}{dz} [I_{0L}(z) S_{\text{ISS}}(z)]. \quad (11)$$

A similar procedure has also been very recently applied by Constantinescu [12] to a measurement in which I_0 was varied and the aperture held fixed at $z=0$.

Using the above routine we are able to easily obtain $N(I)$ at the particular on-axis intensity values spanned by the z positions of our measurements. This requires measurements at several positions, each made with sufficient statistics, in order to map the behavior of $N(I)$ with intensity. This is necessary since the inversion procedure involves differentiation of the signal, which exaggerates statistical errors in the result. Fortunately it is possible to collect enough data to surmount this problem with the current experimental setup and the high repetition rate of the laser system. In order to increase confidence in these results it is also necessary to have a well-characterized focus. We have measured the intensity distribution of the focus and found it to be well described as Gaussian. Additionally, it is possible to determine I_{0L} vs z carefully by examining photoelectron kinetic-energy spectra. Peaks that appear abruptly in the spectra at very specific resonance intensities can act as markers for calibration of the intensity scale with a good degree of accuracy [13].

As an example of the deconvolution procedure, we present in Fig. 2, data from the experiment by Hansch *et al.* [9], which measured intensity-dependent multiple ionization of xenon. Figure 2(a) shows the raw data, which is the number of xenon ions of each charge state measured versus the z position of the pinhole, where $z=0$ is at the minimum beam waist. The rollover in the number of singly charged ions, due to their depletion by double ionization, is a signature of the limited extraction volume [5]. Similar effects have also been observed in experiments where the volume was restricted and the peak intensity varied [12,14]. Figure 2(b) shows the data after inversion and scaling for the relative detection sensitivity for different charge states. These curves represent

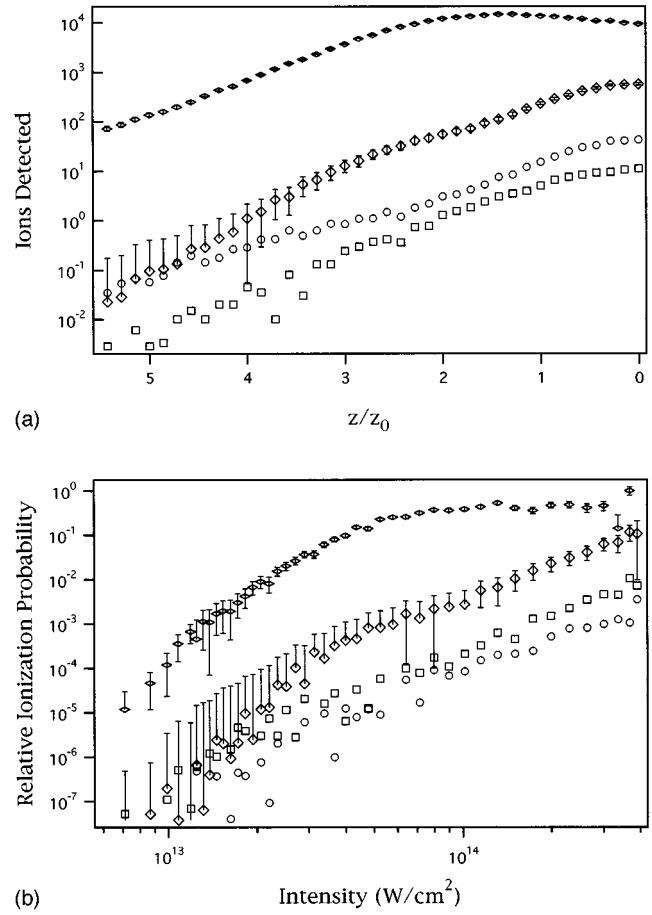


FIG. 2. Multiple-ionization data for xenon in its original (a) and inverted (b) forms. Data have been corrected for detection sensitivity using the method described in the text.

$N_i(I)$, the relative number of ions of the i th charge state ($i = 1$ to 4) per unit volume produced at intensity I . The number of singly charged ions saturates around 7×10^{13} W/cm² and does not increase beyond this point. This is expected, since the probability for ionization has a maximum value of unity. The slope of the curve becomes slightly negative at the highest intensities with the onset of depletion by double ionization. The occurrence of nonsequential double ionization (NSDI) is clearly evident in the Xe²⁺ curve, which shows significant double ionization before the Xe⁺ saturation intensity, as well as a change in slope near 9×10^{13} W/cm². Here the dominant process changes from nonsequential to sequential ionization. The curves for Xe³⁺ and Xe⁴⁺ are less dependable due to a lack of statistics in their collection, but are shown for completeness.

Since all geometric dependencies have been removed from the data, it is possible to calibrate the ion yields for relative detection efficiencies. The sum of the different charge states is required to be unity for intensities above the saturation intensity. It should be possible, in fact, to absolutely calibrate the detection efficiency using data with better statistics due to the probability for ionization having an absolute maximum of unity.

To examine the reliability of our procedure, we have included error bars on the curves for singly and doubly charged xenon. These represent an estimate of the maximum

likely error due to the propagation of statistical errors in the original signal through the deconvolution routine, and two general remarks can be made regarding them. First, because the algorithm involves differentiation, statistical fluctuations in the data can result in negative values in $N(I)$, which are unphysical and have been removed from the data shown. Second, the error in $S(z)$ is, as expected, amplified in $N(I)$, especially for those points taken where dI_{0L}/dz is small, namely in the center and the far wings of the focus. However, both problems are found to converge fast enough to be surmountable by simply collecting enough data. We have not included systematic errors in the analysis, as they are specific to an experiment, and we are interested in examining properties of the inversion method itself. They can be minimized by accurate measurement of the intensity as previously described. In short, the fundamental limitations of the method are experimental; it is reliable when used with data from experiments done carefully and with sufficient statistics,

which is realizable with high-repetition-rate laser systems.

The measurement of intensity dependence in strong-field laser-matter interactions continues to be an important tool as experiments extend into the realm of molecular ionization and dissociation. We have shown that it is possible to convert experimental ionization data to probability distributions. In this form, the results are more representative of fundamental physics and better suited for comparison to theory. This simple procedure is made possible by restricting the detection volume and utilizing intensity-selective scanning to vary the local peak intensity. Future use of this method will afford a clearer understanding of ionization probabilities in atoms, ions, and molecules by allowing the physics of these processes to be directly represented.

This material is based upon work supported by the U.S. Army Research Office under Grant No. DAAH04-95-1-0418.

-
- [1] A. Talebpour *et al.*, J. Phys. B **29**, 5725 (1996).
 - [2] R. R. Jones, Phys. Rev. Lett. **74**, 1091 (1995).
 - [3] R. Jones, Phys. Rev. Lett. **75**, 1491 (1995).
 - [4] R. R. Jones, Laser Phys. **7**, 733 (1997).
 - [5] P. Hansch *et al.*, Phys. Rev. A **54**, R2559 (1996).
 - [6] P. Hansch and L. D. Van Woerkom, Opt. Lett. **21**, 1286 (1996).
 - [7] K. J. Schafer and K. C. Kulander, Laser Phys. **7**, 740 (1996).
 - [8] G. N. Gibson *et al.*, Phys. Rev. A **49**, 3870 (1994).
 - [9] P. Hansch *et al.*, Phys. Rev. A **54**, R2559 (1996).
 - [10] R. P. Kanwal, *Linear Integral Equations* (Academic, New York, 1971).
 - [11] The Liebniz rule states that $(d/dx) \int_{\alpha(x)}^{\beta(x)} F(x,y) dy = \int_{\alpha(x)}^{\beta(x)} (\partial F / \partial x)(x,y) dy + F(x,\beta)(\partial \beta / \partial x) - F(x,\alpha)(\partial \alpha / \partial x)$.
 - [12] R. C. Constantinescu, Ph.D. dissertation, FOM Institute for Atomic and Molecular Physics, 1997 (unpublished).
 - [13] P. Hansch *et al.*, Phys. Rev. A **57**, 709 (1998).
 - [14] D. Charalambidis *et al.*, Phys. Rev. A **50**, R2822 (1994).